Joint constraints on relativistic jets from neutron star mergers

A thesis submitted

in partial fulfillment for the award of the degree of

Master of Science

in

Astronomy and Astrophysics

by

B.S.Bharath Saiguhan

Department of Earth and Space Sciences
Indian Institute of Space Science and Technology
Thiruvananthapuram, India

May 17, 2021

Certificate

This is to certify that the thesis titled ***Joint constraints on relativistic jets from neutron star mergers*** submitted by **B.S.Bharath Saiguhan**, to the Indian Institute of Space Science and Technology, Thiruvananthapuram, in partial fulfillment for the award of the degree of **Master of Science** in **Astronomy and Astrophysics** is a bona fide record of the original work carried out by him/her under my supervision. The contents of this thesis, in full or in parts, have not been submitted to any other Institute or University for the award of any degree or diploma.

Dr. Resmi Lekshmi
Designation

Name of Department Head
Designation

Place: Thiruvananthapuram
Date: May 17, 2021

Declaration

I declare that this thesis titled ***Joint constraints on relativistic jets from neutron star mergers*** submitted in partial fulfillment for the award of the degree of **Master of Science** in **Astronomy and Astrophysics** is a record of the original work carried out by me under the supervision of **Dr. Resmi Lekshmi**, and has not formed the basis for the award of any degree, diploma, associateship, fellowship, or other titles in this or any other Institution or University of higher learning. In keeping with the ethical practice in reporting scientific information, due acknowledgments have been made wherever the findings of others have been cited.

Place: Thiruvananthapuram
Date: May 17, 2021

B.S.Bharath Saiguhan
(SC16B123)

This thesis is dedicated to ...

Acknowledgements

I acknowledge ...

B.S.Bharath Saiguhan

Abstract

Abstract here.

Contents

List of Figures

List of Tables

List of Algorithms

Abbreviations

GNU	GNU's Not Unix
EMACS	Editor MACroS

Nomenclature

m	Mass of the object
c	Velocity of light

Chapter 1

Introduction

1.1 Outflows from BNS Mergers

Due to the joint electromagnetic and gravitational wave detection of the binary neutron star coalescence known as GW1701817 (see [1]), there has been renewed interest in sGRBs. Specifically, the claim that SGRBs have binary neutron star mergers as their central engines (see [2]) gained credence because of this detection. There are other aspects of the process that are not as clear. Specifically, several aspects of GW170817 have not been completely explained. The main concerns are as follows [3]:

- The outflow of GRB170817A was lower in energy, compared to that of a typical cosmological SGRB, by a factor of $10^4 - 10^5$, even though the event was one of the closest GW events recorded, at a distance of ~ 40 Mpc. This could be due to two factors :
  - The observer being off-axis with respect to the structured jet.
  - The internal engine powering this SGRB was intrinsically less energetic, and differs from the one observed in other typical SGRBs.
- A clear consensus has not been reached on how the gamma-ray prompt emission was produced. The uncertainty partly comes from the fact that the various delays involved before the prompt emission is observed are not accurately constrained. Models which have been considered include :
  - The structured outflow model, characterised by functions for the Lorentz factor and the energy per unit solid angle, both of which vary with the

angle made with the polar jet axis (θ). This model produces detectable signals even at moderately large off-axis angles.

- The shock breakout model, wherein the leading edge of the wind emits the prompt emission as it breaks out of the cocoon of nuclear matter ejected before the jet was launched. This model has been shown to explain the energetics and spectrum of the prompt emission, although it does require a setup in which the wind is fast enough so that it can reach a large enough distance at breakout.

More light can be shed on these questions by observing more such SGRBs, using both the gravitational wave (GW) and electromagnetic (EM) windows. However, the possibility of joint detections are slim, due to the fact that the EM observations are highly dependent on the viewing angle of the system with respect to the observer (due to relativistic beaming), whereas GW signal amplitudes depend on the distance to the event [4].
Given that this is the case, it is expedient to look for constraints on the structure parameters of various models. Furthermore, it is useful to develop models which are resilient to non-detections, and can produce constraints on the parameters using upper limits on the flux/fluence observed by the various EM follow-up satellites, such as INTEGRAL, Fermi or Swift.

As mentioned before, the electromagnetic follow-up of the binary neutron star merger event GW170817 helped measure the various time delays between the time of the GW signal trigger (which roughly is the merger time itself) and the time the gamma-ray signals were picked up. This time delay is denoted $\Delta t_{GW-\gamma}$, and was around 1.75 seconds for this event. The components which make up this delay are as follows [3]:

- **Engine Delay** : this is the delay due to some transition mechanism in the central engine which powers the jet (such as a metastable, fast spinning neutron star which collapses into a black hole when its rotation period increases; this process can take years) or due to the need of amplifying the magnetic field to a value large enough to launch the jet (this process is significantly faster, taking seconds). This is denoted by Δt_{eng}.

- **Wind Delay** : this is simply a delay in the launching of a non-relativistic wind due to the neutron-rich matter from the progenitors being tidally shredded. For

this reason, it can be *negative* as well, since the tidal shredding can occur before the merger itself. This is denoted as Δt_{wind}.

- **Breakout Delay** : if the wind is ejected before the jet, then the latter will have to propagate through the former and this happens at a sub-relativistic speed, whereas the GW signal travels at a relativistic speed. The delay due to this crossing is the breakout delay, and is denoted Δt_{bo}. During this time, jet-wind interactions cause the development of a structured outflow that maintains a bright core but also has energetic wings at large polar angles.

- **Photospheric Delay** : once the jet has crossed the wind, it still needs to propagate out to the photospheric radius, where the outflow becomes transparent and the prompt gamma-ray emission is radiated. The delay from the breakout radius to the photospheric radius is Δt_{ph}. This is given as (for GW170817):

$$\Delta t_{ph} \sim \frac{R_{ph}}{c\Gamma^2} = 1.4 \frac{R_{ph}}{2 \times 10^{12}\ \mathrm{cm}} \left(\frac{7}{\Gamma}\right)^2\ \mathrm{s} \tag{1.1}$$

- **Dissipation Delay** : this is a requirement in some models, such as the internal shock synchrotron model, wherein the outflow needs to travel to the internal shock radius before the bulk energy of the flow is dissipated and turned into radiation. The time required to get to this point after crossing the photospheric radius is the dissipation delay, denoted Δt_{γ}

Several attempts to constrain the various time delay components have been made. However, except for relative comparisons, no conclusions have been arrived upon. For example, one can only say that the photospheric delay is the major component out of all the delays, and that wind delay (if non-zero) has to be lesser than the jet delay, so that the jet catches up to the wind and the jet-wind interaction generates the structured outflow. The figure below summarises these delays in the broader context.

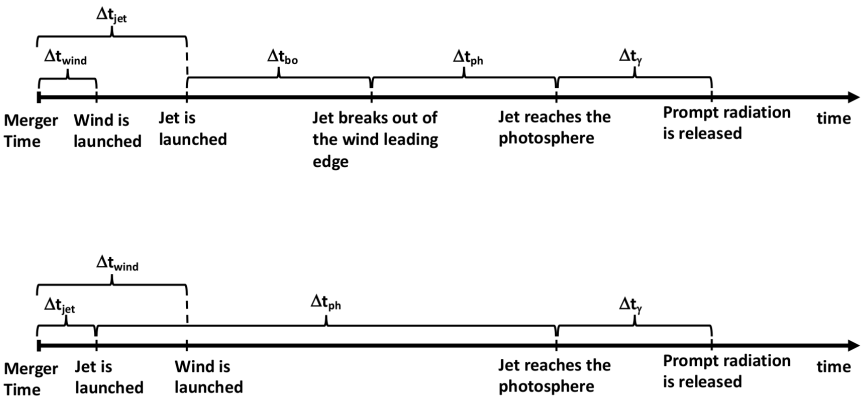

Figure 1.1: Two possible scenarios for the relative positioning of the delays in time, which contribute to $\Delta t_{GW-\gamma}$. Owing to the requirement of a structure outflow, GW170817 possibly follows the top timeline. The relative contributions of the various delays are debated, but it is agreed that $\Delta t_{wind} < \Delta t_{jet} \ll 1$ s, $\Delta t_{bo} \ll 1$ s, $\Delta t_{\gamma} \sim 0$ and $\Delta t_{ph} \sim \Delta t_{GW-\gamma}$.

Due to the uncertainties in the delay terms, several models for the jet can explain the energetics and observed structure. Numerical simulations are also not unequivocal about their favouring of one model over the other (see [5]). Some models try to explain the apparent structure of the jet, that is the observables seen by a particular observer at a particular viewing angle. Other models are used to explain the *intrinsic* structure, such as the polar angle variation of the bulk Lorentz factor and the energy across the solid angle, in the jet co-moving frame (see [6] for a detailed discussion of the differences between the two structures). Some of these are given below (see also Figs. 1.2 and 1.3):

- Top-hat : This model, as used in [7], assumes that the bulk Lorentz and energy functions drop to zero beyond some cutoff angle, θ_j. Below this threshold, the functions are at their respective on-axis values.

- Gaussian : This model is widely used, in some contexts to explain the apparent jet structure (by [8]), and in others the intrinsic jet structure (by [7]). The former is simply given by $y_{GJ}(\theta) = e^{-\frac{1}{2}\left(\frac{\theta}{\theta_\sigma}\right)^2}$, since the authors consider only the apparent jet structure, as explained above and θ_σ is a structure parameter which is inferred by the authors' Bayesian inference.
  In the latter, as the authors consider the intrinsic jet structure, they assume

that $\Gamma\beta(\theta) = \Gamma_0\beta_0 \exp(-\theta^2/2\theta_c^2)$ and that $\epsilon(\theta) \propto \exp(-\theta^2/\theta_c^2)$[1], and derive the observed properties (see below).

- Power Law : This model is used by [8] to explain the apparent structure of the jet, assuming that any variation in the energy is simply because of relativistic beaming and the jet being viewed off-axis. It is given using the shape function $y(\theta)$ (which is multiplied with the on-axis isotropic equivalent energy $E_{iso,0}$ to give $E_{iso}(\theta)$[2]):

$$y(\theta) = \begin{cases} 1, & 0 \leq \theta \leq \theta_c, \\ (\theta/\theta_c)^{-2}, & \theta_c < \theta \leq \theta, \\ 0, & \theta_j < \theta \end{cases} \tag{1.2}$$

  Here θ_c and θ_j are simply structure parameters, inferred using Bayesian methods.

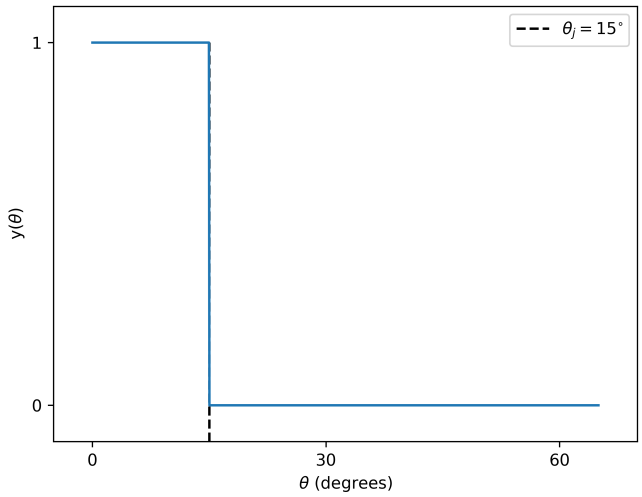

Figure 1.2: Functional form of the tophat jet structure model, as considered in [7]. The dashed line denotes the jet angle $\theta_j = 15^\circ$.

[1]This is the normalised energy profile function. The normalisation constant is estimated by the condition $2\pi \int d(\cos\theta)\epsilon(\theta) = E_{tot.,\gamma}$, where $E_{tot.,\gamma}$ is the total energy in gamma-rays.

[2]Using the equation $E_{iso}(\theta_v) = E_{iso,0} \cdot y(\theta_v)$

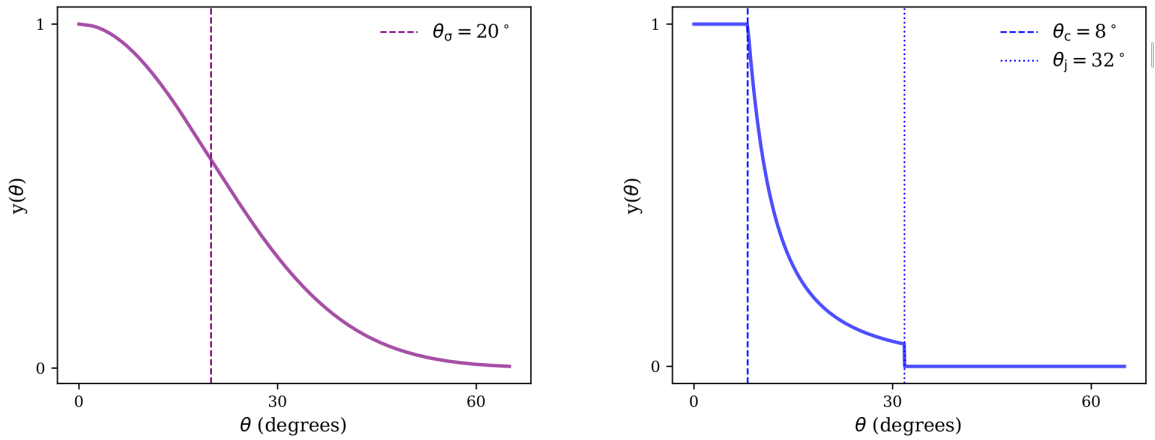

Figure 1.3: Functional forms of the jet structure models, as considered by [8]. (Left) The gaussian jet structure with a width $\theta_\sigma = 20°$, also marked by the dashed line. (Right) The power-law structure with a core angle $\theta_c = 8°$ and a jet angle $\theta_j = 32°$.

In order to start off with an intrinsic structure and calculate the observed structure, following [9], we start off by considering the emission profile of a point source moving at some angle with the observer, essentially rendering this scenario off-axis. This will affect the prompt jet emission, as well as the initial afterglow, and so warrants careful analysis. Now, let the initial jet opening angle be θ_0 and let the observer be at an angle θ_{obs}. In general, for a point source moving at any angle θ with respect to the observer, the observed flux is given by :

$$F_\nu = \frac{L'_{\nu'}}{4\pi d_L^2}\left(\frac{\nu}{\nu'}\right)^3 = \frac{1+z}{4\pi d_L^2}\frac{L'_{\nu'}}{\gamma^3(1-\beta\cos\theta)^3} \tag{1.3}$$

Here, $L'_{\nu'}$ and ν' are the jet comoving frame spectral luminosity and frequency, d_L is the luminosity distance, $\gamma = (1-\beta^2)^{-1/2}$ is the jet Lorentz factor. If t and ν are the observed time and frequency for an observer at θ, and t_0 and ν_0 are those for an observer on the axis, then:

$$\frac{t_0}{t} = \frac{\nu}{\nu_0} = \frac{(1-\beta)}{(1-\beta\cos\theta)} \equiv a \approx \frac{1}{(1+\gamma^2\theta^2)} \tag{1.4}$$

And finally putting Eq. 1.4 into Eq. 1.3 and expanding using a Taylor series approximation upto the leading order:

$$F_\nu(\theta_{obs}, t) = a^3 F_{\nu/a}(0, at) \tag{1.5}$$

This gives us a handle on how to relate observed off-axis quantities to the on-axis

ones. Furthermore, this enables us to go from an intrinsic structure to an observed one, which is what was required.

1.2 Outflows from NSBH Mergers

The difference in this pathway to sGRBs, compared to the case of BNS mergers, is that though there is theoretical and simulational support for the launching of sGRB jets from the merger of a neutron star and a black hole of appropriate mass (see for example **citations**), there has not been strong evidence from the observational side of things. In the first half of the third observing run of the LVC (also known as O3a), there have been several triggers which have been reportedly confident NSBH triggers. However, there were no counterpart EM signals picked up, which decreases the credibility of NSBH mergers as the progenitors of sGRBs.

The electromagnetic component from NSBH mergers, is largely decided based on the amount of mass left post-merger, outside the horizon of the black hole. This decides how much matter participates in the subsequent processes, which may be the rapid neutron-capture process which gives rise to the kilonova signal or the magnetic field amplification via magneto-rotational instability which leads to a sGRB jet.

Qualitatively, for a binary where the neutron star is treated as a test mass and the black hole's spin is aligned with the orbital angular momentum of the binary, the innermost-stable circular orbit radius r_{ISCO} scales as $r_{ISCO} \sim f(\chi_{BH})GM_{BH}/c^2$ (where f is a function ranging from 1 to 9, decreasing for increasing (prograde) spins; see [10]) and the radius at which the tidal disruption of the neutron star starts, r_{dis} scales as $r_{dis} \sim k(M_{BH/M_{BNS}})^{1/3}R_{NS}$ (where k is a constant with a dependence on the black hole spin and the equation of state). Only requiring that $r_{dis} \gtrsim r_{ISCO}$, as a rough requirement for disruption to occur before the neutron star plunges into the black hole, leads to the conclusion that (a.) low-mass black holes (b.) larger NS radii (c.) higher prograde black hole spins favour disruption. This is seen as well from Fig. 1.7. However, the actual quantitative results need to be simulated such the effect of the various components in the problem are correctly taken into account. As seen from carrying these simulations out, the matter left over post-merger heavily depends on (for a summary, see Fig. 1.6):

- The mass ratio of the system. This is defined as $q = M_{BH}/M_{NS}$ so that $q > 1$

always. Fully general relativistic, magnetohydrodynamic simulations (such as [11]) show that in cases where the mass ratio is 3:1, regardless of the neutron spin, a collimated outflow is observed, whereas the same is not realised in cases where the mass ratio is 5:1 or higher.

- The spin of the components of the system. In geometrized units (where $G = c = 1$), these are prescribed in terms of a_{BH}/M_{BH} or a_{NS}/M_{NS}, and whether these two spins align (prograde) or are anti-aligned (retrograde) decides whether the neutron star would be tidally disrupted, and hence participate in the processes mentioned previously, or not. Via simulations, it is seen that the more the prograde spin of the neutron star, the farther out the neutron star is tidally disrupted, albeit this is only observed for the case of q = 3:1 (comparing say, Figs. 1.4 and 1.5). Also, this leads to long tidal tails, which produces a baryon-loaded environment and thus the magnetic field of the tidally disrupted matter must overcome the baryon ram pressure to launch the jet. This process hence delays the launching of the jet.

Aside from the sGRB jet, which requires magnetic field amplification (via MRI) as well as thermal pair production (from the disk remnant) followed by the Blandford-Znajek process, there is a possibility that NSBH mergers can produce kilonovae signatures. For this, the dynamically ejected mass has to be between $10^{-4.5} - 10^{-2}(M_{NS}/1.4M_{\odot})M_{\odot}$ (see [11] for more details), and this will lead to kilonovae potentially detectable by the Large Synoptic Survey Telescope (LSST).

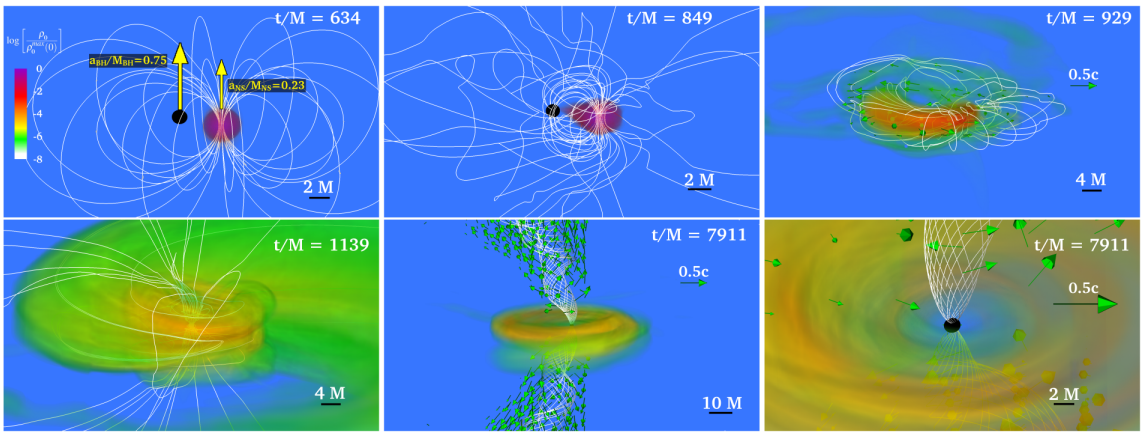

Figure 1.4: Volume rendering of the rest mass density (ρ_0) (in log scale), normalized to the NS maximum value $\rho_0 = 8.92 \times 10^{14} (1.4 M_\odot / M_{NS})^2$ g/cm^3, for particular times for a magnetized neutron star, with q = 3:1 and a prograde NS spin of 0.23. Top three panels highlight the inspiral and the tidal disruption, whereas the bottom three panels highlight the appearance of the magnetically-driven jet. White lines denote the magnetic field, arrows denote the fluid velocity and the BH's apparent horizon is the black sphere. Here M $= 2.5 \times 10^{-2} (M_{NS}/M_{1.4M_\odot})$ ms $= 7.58 (M_{NS}/M_{1.4M_\odot})$ km (in geometrized units). From [11].

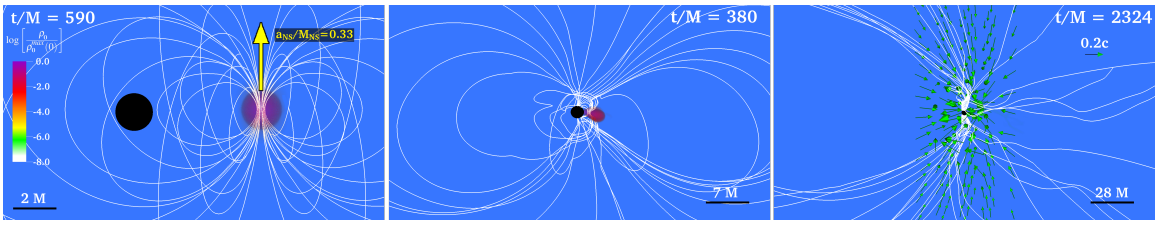

Figure 1.5: Similar to Fig. 1.4, however with the NS spin being 0.33, the BH spin being 0 and q = 5:1. In this case, no strong collimation of the magnetic field is observed from the merger remnant, and so a magnetically-driven jet is also not observed. From [11].

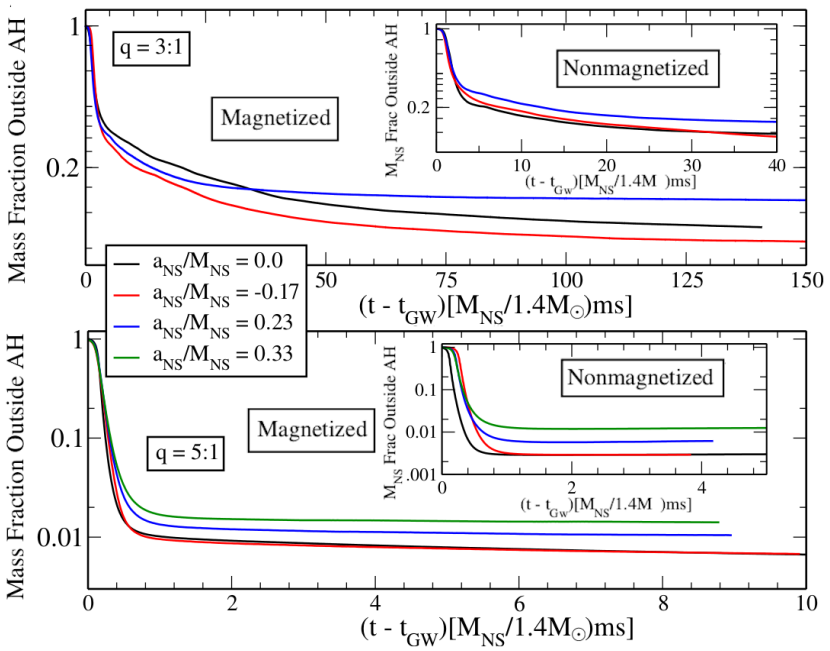

Figure 1.6: Fraction of rest-mass of the NS outside the apparent horizon of the black hole as a function of coordinate time, for the various configurations considered in [11]. The inset figures report the same for non-magnetized cases, and the coordinate time is shifted such that the merger time coincides with 0.

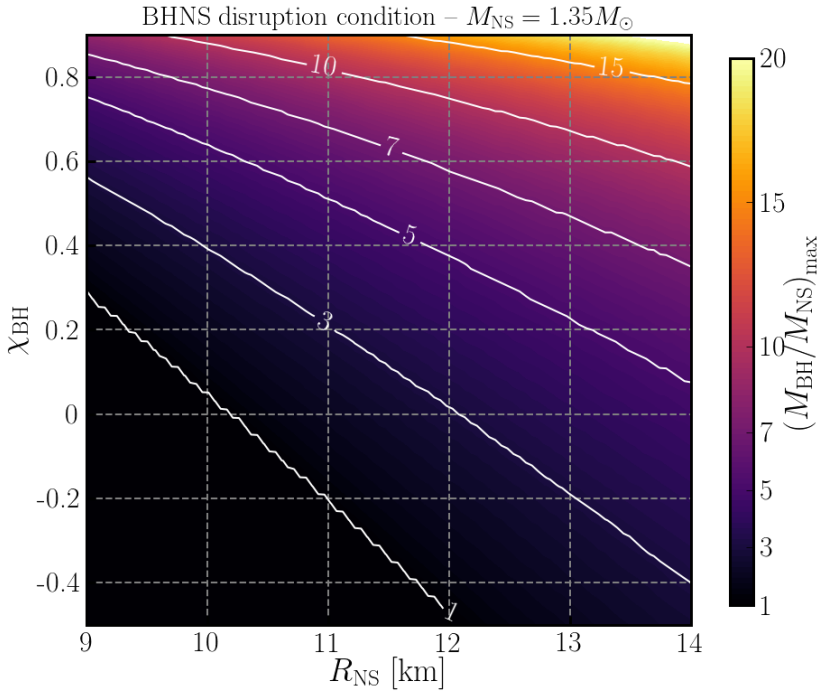

Figure 1.7: Maximum value of the mass-ratio (M_{BH}/M_{NS}) for which a NSBH system disrupts, as a function of the neutron star radius R_{NS}, and the aligned component of the dimensionless black hole spin χ_{BH}, assuming $M_{NS} = 1.35 M_\odot$. Results for other neutron star masses can be obtained by rescaling considering the disruption condition at constant compaction $C_{NS} = GM_{NS}/R_{NS}c^2$. From [12].

Chapter 2
Related Work

Write related work here.

2.1 Summary

Chapter 3
Conclusions

Conclusions here.

References

1. Abbott, B. P. *et al.* GW170817: Observation of Gravitational Waves from a Binary Neutron Star Inspiral. *Physical Review Letters* **119,** 161101. ISSN: 0031-9007, 1079-7114. https://link.aps.org/doi/10.1103/PhysRevLett.119.161101 (2020) (Oct. 16, 2017).

2. Narayan, R., Paczynski, B. & Piran, T. Gamma-ray bursts as the death throes of massive binary stars. *The Astrophysical Journal* **395,** L83. ISSN: 0004-637X, 1538-4357. http://adsabs.harvard.edu/doi/10.1086/186493 (2020) (Aug. 1992).

3. Lazzati, D. Short duration gamma-ray bursts and their outflows in light of GW170817. *arXiv:2009.01773 [astro-ph].* arXiv: 2009.01773. http://arxiv.org/abs/2009.01773 (2020) (Sept. 3, 2020).

4. Saleem, M. Prospects of joint detections of neutron star mergers and short-GRBs with Gaussian structured jets. *Monthly Notices of the Royal Astronomical Society* **493,** 1633–1639. ISSN: 0035-8711, 1365-2966. arXiv: 1905.00314. http://arxiv.org/abs/1905.00314 (2020) (Apr. 1, 2020).

5. Shibata, M. & Hotokezaka, K. Merger and Mass Ejection of Neutron-Star Binaries. *Annual Review of Nuclear and Particle Science* **69,** 41–64. ISSN: 0163-8998, 1545-4134. arXiv: 1908.02350. http://arxiv.org/abs/1908.02350 (2020) (Oct. 19, 2019).

6. Salafia, O. S., Ghisellini, G., Pescalli, A., Ghirlanda, G. & Nappo, F. Structure of gamma-ray burst jets: intrinsic versus apparent properties. *Monthly Notices of the Royal Astronomical Society* **450,** 3549–3558. ISSN: 1365-2966, 0035-8711. http://academic.oup.com/mnras/article/450/4/3549/989952/Structure-of-gammaray-burst-jets-intrinsic-versus (2020) (July 11, 2015).

7. Saleem, M., Resmi, L., Arun, K. G. & Mohan, S. On the energetics of a possible relativistic jet associated with the binary neutron star merger candidate S190425z. *The Astrophysical Journal* **891,** 130. ISSN: 1538-4357. arXiv: 1905.00337. http://arxiv.org/abs/1905.00337 (2020) (Mar. 12, 2020).

8. Hayes, F., Heng, I. S., Veitch, J. & Williams, D. Comparing Short Gamma-Ray Burst Jet Structure Models. *The Astrophysical Journal* **891,** 124. ISSN: 1538-4357. arXiv: 1911.04190. http://arxiv.org/abs/1911.04190 (2020) (Mar. 12, 2020).

9. Granot, J., Panaitescu, A., Kumar, P. & Woosley, S. E. Off-Axis Afterglow Emission from Jetted Gamma-Ray Bursts. *The Astrophysical Journal* **570,** L61–L64. ISSN: 0004637X, 15384357. https://iopscience.iop.org/article/10.1086/340991 (2020) (May 10, 2002).

10. Bardeen, J. M., Press, W. H. & Teukolsky, S. A. Rotating Black Holes: Locally Nonrotating Frames, Energy Extraction, and Scalar Synchrotron Radiation. *Astrophysical Journal* **178,** 347–370 (Dec. 1972).

11. Ruiz, M., Paschalidis, V., Tsokaros, A. & Shapiro, S. L. Black hole-neutron star coalescence: effects of the neutron star spin on jet launching and dynamical ejecta mass. *arXiv:2011.08863 [astro-ph, physics:gr-qc].* arXiv: 2011.08863. http://arxiv.org/abs/2011.08863 (2020) (Nov. 17, 2020).

12. Foucart, F. A brief overview of black hole-neutron star mergers. *arXiv:2006.10570 [astro-ph, physics:gr-qc].* arXiv: 2006.10570. http://arxiv.org/abs/2006.10570 (2020) (June 18, 2020).